

Light Meson Decays from Photon-Induced Reactions with CLAS

Michael C. Kunkel^{1,a)} and for the CLAS Collaboration

¹*Forschungszentrum Jülich, Jülich (Germany)*

^{a)}m.kunkel@fz-juelich.de

Abstract. Photo-production experiments with the CEBAF Large Acceptance Spectrometer (CLAS) at the Thomas Jefferson National Laboratory produce data sets with unprecedented statistics of light mesons. With these data sets, measurements of transition form factors for η , ω , and η' via conversion decays can be performed using a line shape analysis on the invariant mass of the final state dileptons. Tests of fundamental symmetries and information on the light quark mass difference can be performed using a Dalitz plot analysis of the meson decay. An overview of the first results and future prospects within the newly upgraded CLAS apparatus will be given.

INTRODUCTION

Decays of light mesons provide insight into the structure of the meson. The Light Meson Decay (LMD) group, established at the Thomas Jefferson National Facility with worldwide collaboration, investigates physics pertaining to, but not limited to, transition form factors, anomalous decays and the search for CP violation through Dalitz plot analysis. The presentation given was an overview of the LMD program, recent updates on measurements and an outlook on measurements that can be taken with the CLAS12 detector.

Light Meson Decay Program

The light meson group was established in 2013. The goal of the group is to investigate properties of light meson decays using data obtained from the CLAS detector. Figure 1 shows the CLAS detector and its sub components. Since decays

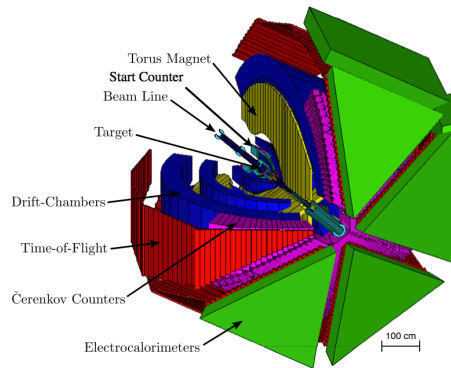


FIGURE 1: The CEBAF Large Acceptance Spectrometer (CLAS)

of hadrons are independent of production, all CLAS data can be used, however there are two experiments that were chosen as flagships for the program, the g11 and g12 experiment. Both experiments use a photon beam incident on a

liquid hydrogen target which created photo-induced reactions, 800 MeV - 3.8 GeV for g11 and 1.1 GeV - 5.5 GeV for g12. See Table 1 for a list of meson decays the LMD group plans to investigate.

TABLE 1: LMD planned measurements

Meson Decay	Physics Interest	Meson Decay	Physics Interest
$\pi^0 \rightarrow e^+e^-\gamma$	Heavy photon upper limit	$\eta' \rightarrow \pi^+\pi^-\gamma$	Box anomaly
$\eta' \rightarrow e^+e^-\gamma$	Transition form factor	$\omega \rightarrow \pi^+\pi^-\gamma$	Upper limit branching ratio
$\omega \rightarrow e^+e^-\pi^0$	Transition form factor	$\eta, \omega, \phi \rightarrow \pi^+\pi^-\pi^0$	Dalitz plot analysis
$\eta' \rightarrow e^+e^-\pi^0$	C violation	$\eta' \rightarrow \pi^+\pi^-\eta^0$	Dalitz plot analysis
$\eta' \rightarrow e^+e^-\pi^+\pi^-$	CP violation	$\phi \rightarrow \pi^+\pi^-\eta^0$	G-parity violation

Update on the Radiative decay of the η and η' meson

The 2 photon decay of pseudoscalar mesons $\pi^0, \eta, \eta' \rightarrow \gamma\gamma$ proceed from the understood triangle or axial anomaly. While radiative decays of $\eta, \eta' \rightarrow \pi^+\pi^-\gamma$ are related to a less understood box anomaly. Figure 2 shows the Feynman diagrams for the two processes previously described. The radiative decay widths of η' and η are determined by the

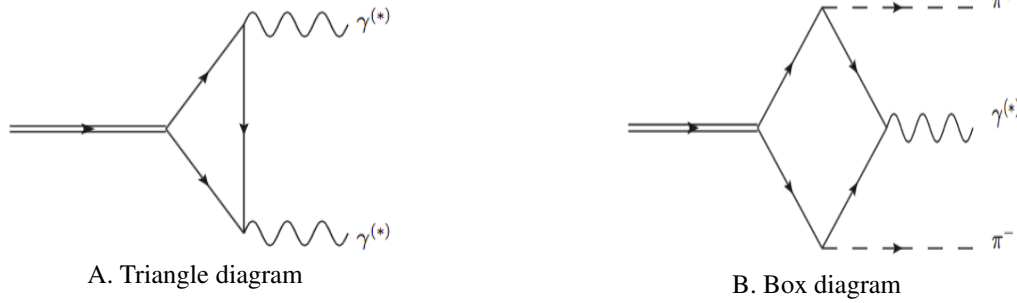


FIGURE 2: Feynmann diagram of the two photon decay (A). Feynmann diagram of the axial anomoly, box diagram (B)

box anomaly in the chiral limit by use of equation 1.

$$\frac{d\Gamma(\eta^{(\prime)} \rightarrow \pi^+\pi^-\gamma)}{ds_{\pi\pi}} = A|P(s_{\pi\pi})F_V(s_{\pi\pi})\Gamma_0(s_{\pi\pi})| \quad (1)$$

Where $\Gamma_0(s_{\pi\pi})$ is the P-wave phase-space constant, denoted in equation 2 with κ being a numerical constant. $F_V(s_{\pi\pi})$ is the pion form factor that can be approximated by the equation 3 and $P(s_{\pi\pi})$ is expanded in the chiral limit, $s_{\pi\pi} = 0$, and is written in equation 4, where α is the variable of measurement.

$$\Gamma_0(s_{\pi\pi}) = \frac{\kappa (M_{\eta^{(\prime)}}^2 - s_{\pi\pi})^3 s_{\pi\pi} \left(1 - \frac{4M_\pi^2}{s_{\pi\pi}}\right)^{\frac{3}{2}}}{M_{\eta^{(\prime)}}^3} \quad (2)$$

$$|F_V(s_{\pi\pi})| \approx 1 + (2.12 \pm 0.01)s_{\pi\pi} + (2.13 \pm 0.01)s_{\pi\pi}^2 + (13.89 \pm 0.14)s_{\pi\pi}^3 \quad (3)$$

$$P(s_{\pi\pi}) = 1 + \alpha s_{\pi\pi} + \mathcal{O}(s_{\pi\pi}^2) \quad (4)$$

Previous measurements of the radiative decay for the η meson from WASA-at-COSY [1] and KLOE [2] differ in such a manner that a third measurement is needed, furthermore there exists only one measurement, performed of the η' radiative decay [3]. With the CLAS g11 experiment, both the η and η' radiative decay width will be measured. In

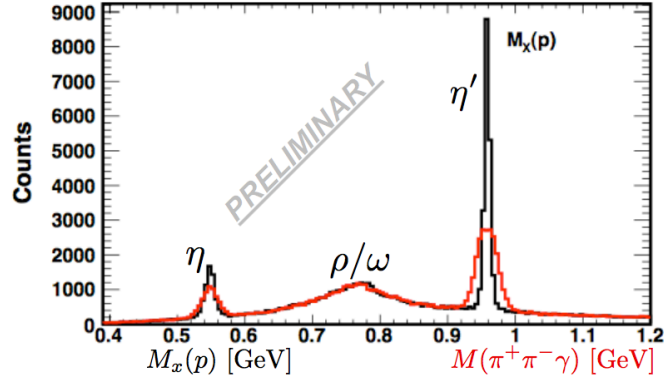


FIGURE 3: CLAS data yield for $\gamma p \rightarrow p\eta^{(\prime)} \rightarrow p\pi^+\pi^-\gamma$ from g11 data set

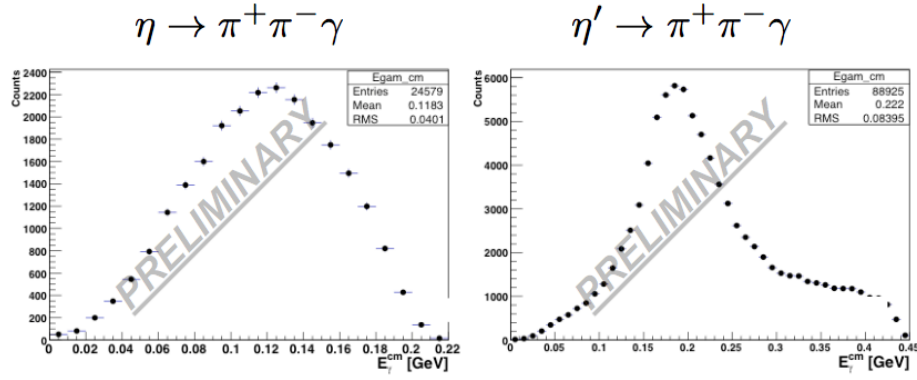


FIGURE 4: CLAS data photon energy distribution for η (left) and η' (right)

figure 3 the CLAS g11 data is shown for the particle selection of exclusive $\gamma p \rightarrow p\pi^+\pi^-\gamma$. Selecting events withing a 2.5σ range of $\eta^{(\prime)}$ the photon energy distribution is shown in figure 4. Visually comparing the shape of the left figure 4 to those of figure 5, for the η meson, and also the right figure 4 to that of figure 6, for the η' meson, it can be seen that the CLAS data is suitable for comparison with previous measurements.

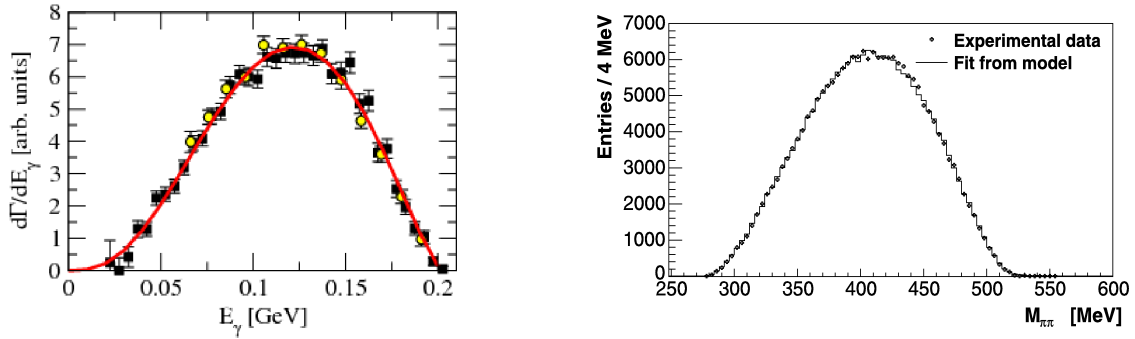


FIGURE 5: WASA-at-COSY data photon energy distribution for η (left) [2] and KLOE data photon energy distribution for η (right)[3].

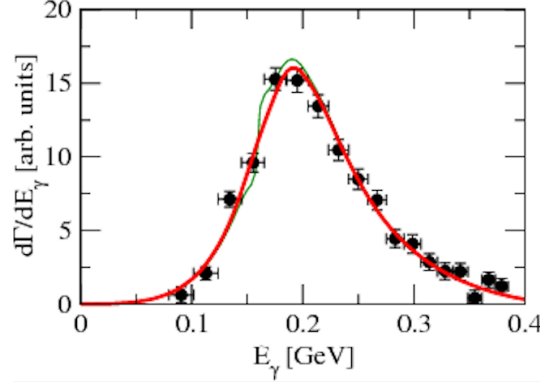


FIGURE 6: CRYSTAL BARREL photon energy distribution for η' [2]

Update on the Dalitz plot analysis of $\eta' \rightarrow \pi^+ \pi^- \eta$

This topic was briefly discussed, as a full update was given by later in the session.

Update on the transition form factor measurement of the ω meson

Transition form factors characterize modifications of the point-like photon-meson vertex due to the structure of the meson. Since the virtual photon can interact with quarks, it can be used as a probe for the internal structure of mesons and its electromagnetic interaction is calculable with the Kroll-Wada formula [4] as seen in equation 5;

$$\frac{d\Gamma_{M \rightarrow l^+ l^- X}}{dq^2 d\Gamma_{M \rightarrow X\gamma}} = \frac{\alpha}{3\pi q^2} \left(\left(1 + \frac{q^2}{m_M^2 - m_X^2} \right)^2 - \frac{4m_M^2 q^2}{(m_M^2 - m_X^2)^2} \right)^{\frac{3}{2}} \left(1 - \frac{4m_l^2}{q^2} \right)^{1/2} \left(1 + \frac{2m_l^2}{q^2} \right) |_{\text{Q.E.D.}} \quad (5)$$

Where M is the species of meson i.e. π^0 , η , ω , η' , etc, X is the daughter particle in the decay, m_M the mass of the meson, m_X the mass of the daughter particle, m_l the mass of the lepton species in the decay, i.e. e^\pm or μ^\pm and q being the e^+e^- or $\mu^+\mu^-$ invariant mass which is equivalent to the mass of the virtual photon. Deviation of equation 5 represents the architecture of the meson and can be incorporated into the transition form factor $|F(q^2)|$. Depending on the lifetime of the meson of interest, the transition can be constructed as a simple pole, equation 6, a complex pole, equation 7, or some other arrangement that describes the transition.

$$|F(q^2)| = \frac{1}{1 - \frac{q^2}{\Lambda^2}} \quad (6)$$

$$|F(q^2)|^2 = \frac{\Lambda^2(\Lambda^2 + \gamma^2)}{(\Lambda^2 - q^2)\Lambda^2\gamma^2}, \quad (7)$$

where Λ and γ is the mass and width of the virtual vector meson mass, respectively. Recent measurements of the transition form factor for $\omega \rightarrow \mu^+\mu^-\gamma$ have shown discrepancy with the Vector Dominance Model [5] and recent models [6] attempt to predict the shape of the virtual vector meson as seen in figure 7. With the CLAS g12 experiment, lepton (e^\pm) identification is done using Cherenkov detectors and electromagnetic calorimetry, providing a $e^+e^-/\pi^+\pi^-$ rejection of 10^6 . Using the e^\pm data from CLAS g12, the $\omega \rightarrow pe^+e^-\pi^0$ transition form factor can be extracted to validate onto the discrepancy. Figure 8 shows the mass section for the ω meson as well as the e^+e^- distribution currently being used to measure the ω transition form factor. Also, the knowledge of the η form factor is needed for the interpretation of the g-2 experiment. Furthermore, the ratio of the η and η' transition form factor provides information into the mixing angle of the combination of the singlet, η_0 , and nonet, η_8 , which are the composites of the η and η' meson.

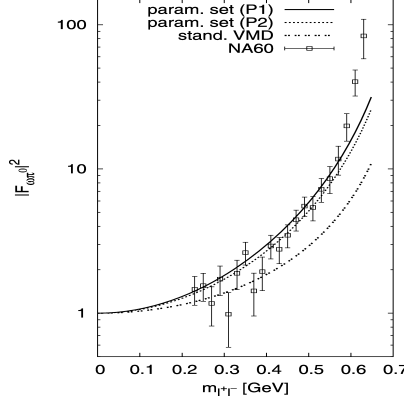


FIGURE 7: Form factor of the decay $\omega \rightarrow l^+l^-\gamma$ compared to dimuon data taken by the NA60 Collaboration [5]. The solid line and dotted line represent recent theoretical models to describe the line shape. The dot-dashed line is calculated with the VMD model equations 5, 7 using the mass of the ρ meson as the virtual vector meson. [6]

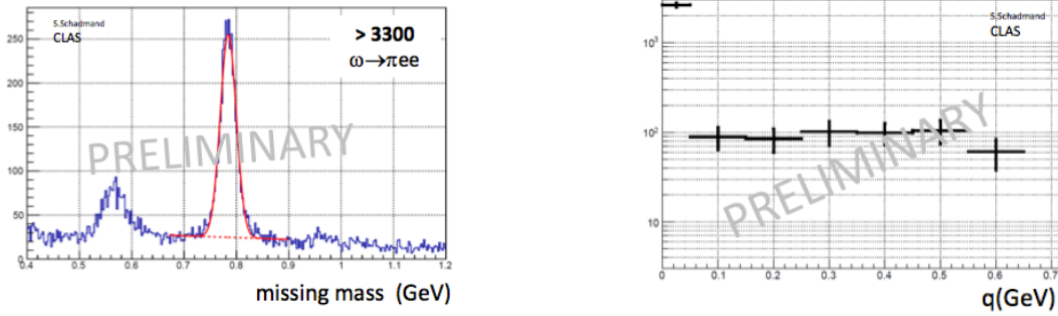


FIGURE 8: CLAS data yield for $\gamma p \rightarrow pX \rightarrow pe^+e^-\pi^0$ from g12 data set (left). $q = e^+e^-$ distribution for events $\gamma p \rightarrow p\omega \rightarrow pe^+e^-\pi^0$ from the g12 data set (right).

Update on the branching ratio measurement of the η' meson $\rightarrow e^+e^-\gamma$

A recent measurement of BESIII reports a branching ratio $\Gamma(\eta' \rightarrow e^+e^-\gamma)/\Gamma(\eta' \rightarrow \gamma\gamma)$ to be $2.13 \pm 0.09(stat.) \pm 0.07(sys.)10^{-2}$ from 864 events [7]. Using the e^\pm data from CLAS g12, preliminarily 89 events of the $\eta' \rightarrow e^+e^-\gamma$ decay were observed and analyzed, using the Q-factor [8] method to suppress background from neighboring $A \rightarrow e^+e^-X$ decays, figure 9. A preliminary branching ratio $\Gamma(\eta' \rightarrow e^+e^-\gamma)/\Gamma(\eta' \rightarrow \gamma\gamma)$ was measured to be $2.63 \pm 0.3(stat.)10^{-2}$, which is consistent with the BESIII measurement. However, the statistics of either BESIII or CLAS are not enough to determine which theoretical model represents the structure of the η' meson, table

Future measurement of the η' meson transition form factor with CLAS12

here

ACKNOWLEDGMENTS

I would like to acknowledge the members of the LMD group for their contributions to the given presentation. Also to the CLAS collaboration.

REFERENCES

- [1] P. Adlarson and et al., Physics Letters B **707**, 243 – 249 (2012).

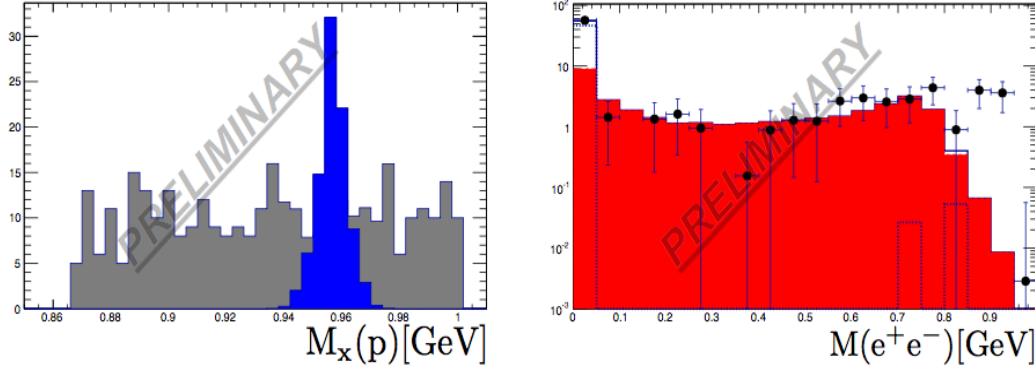


FIGURE 9: CLAS data yield for $\gamma p \rightarrow p\eta' \rightarrow pe^+e^-\gamma$ from g12 data set. Blue peak represents the signal extracted using the Q-factor method, while the gray band represents the background (left). $q = e^+e^-$ distribution for events $\gamma p \rightarrow p\eta' \rightarrow pe^+e^-\gamma$ from the g12 data set. Black points represent data under the blue peak of left plot, while the blue-dashed is simulation of $\eta' \rightarrow \gamma\gamma$ and the red solid area is the simulation of $\eta' \rightarrow e^+e^-\gamma$ (right).

- [2] F. Stollenwerk and et al., Physics Letters B **707**, 184 – 190 (2012).
- [3] D. Babusci and et al., Physics Letters B **718**, 910 – 914 (2013).
- [4] N. M. Kroll and W. Wada, Phys. Rev. **98**, 1355–1359 (1955).
- [5] R. Arnaldi, K. Banicz, J. Castor, B. Chaurand, C. Cical, A. Colla, P. Cortese, S. Damjanovic, A. David, A. de Falco, A. Devaux, L. Ducroux, H. En'yo, J. Fargeix, A. Ferretti, M. Floris, A. Frster, P. Force, N. Guettet, A. Guichard, H. Gulkanian, J. Heuser, M. Keil, C. Lourenco, J. Lozano, F. Manso, P. Martins, A. Masoni, A. Neves, H. Ohnishi, C. Oppedisano, P. Parracho, P. Pillot, T. Poghosyan, G. Puddu, E. Radermacher, P. Ramalhetete, P. Rosinsky, E. Scomparin, J. Seixas, S. Serici, R. Shahoyan, P. Sonderegger, H. Specht, R. Tieulent, G. Usai, R. Veenhof, and H. Whri, Physics Letters B **677**, 260 – 266 (2009).
- [6] C. Terschlusen and S. Leupold, Physics Letters B **691**, 191 – 201 (2010).
- [7] M. Ablikim *et al.* (BESIII), Phys. Rev. **D92**, p. 012001 (2015).
- [8] M. Williams, M. Bellis, and C. A. Meyer, JINST **4**, p. P10003 (2009).
- [9] A. Abele and et al., Physics Letters B **402**, 195 – 206 (1997).